Using MRI To Monitor Tumorigenesis In A Murine Model Of Melanoma Brain Metastasis

A. Morsi^{1,2}, E. Voura^{1,2}, S. Pun², M. Hoang², A. Baig³, E. Parker¹, J. Golfinos¹, and Y. Z. Wadghiri²

¹Neurosurgery, NYU langone medical center, NYC, NY, United States, ²RADIOLOGY, NYU langone medical center, NYC, NY, United States, ³Radiology, NYU langone medical center, NYC, NY, United States

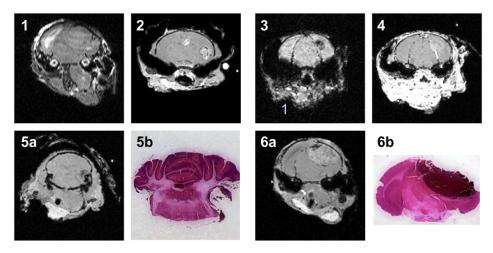
Introduction: Despite aggressive therapies, 95% of patients suffering from melanoma brain metastases succumb to their disease within six months of diagnosis. The abnormal vasculature of these tumors is believed responsible for this poor prognosis. This complicated blood supply limits the delivery of drugs to the cancer cells during chemotherapy and does not provide sufficient oxygenation for successful radiation therapy. Anti-angiogenic drugs are thought to restore a normal blood supply in the tumor by relieving the chaotic flow pattern in the tumor – called vascular normalization (1). Non-invasively following a reliable murine model of melanoma brain metastasis is crucial to better understand the vascular dynamics within these tumors and to assess the vascular changes induced by anti-angiogenic regimens prior to their adaptation to the clinic. We, therefore, aimed to develop a micro-MRI protocol similar those used clinically to monitor the tumorigenesis of B16-F10 melanoma brain metastasis as described by Perides et al. (2).

Methods: Animals & surgery: Experiments were performed on C57black6 mice (WT, N=5). A 100-μl intracarodidal injection of 10⁵ B16-F10 melanoma cells was performed. Tumorigenesis was followed over 4 weeks with serial MRI scans on post-operative day intervals [12-14], [18-20] and [23-26]. Imaging: All μMRI experiments were performed with a 7T Bruker Avance II console (Bruker Biospin, Ettlingen Germany). The protocol consisted of a pre-injection scan to acquire contrast agent-free brain datasets consisting of a pre-T2 weighted 3D-RARE (150 mm x 150 mm x 300 mm; 19-min) to delineate the endogenous effect of edema from the tumor. Pre-T1 weighted and pre-T2* weighted datasets with an identical resolution and imaging time (150 mm³, 30-min) using a modified 3D gradient-echo (GE) sequence were implemented to acquire a self-gated signal on the readout dephasing gradient within each TR (3). The gating signal was retrospectively used for artifact free image reconstruction. This was followed an identical T1-w 3DGE sequence after a femoral injection of Gd Magnevist representing a clinical double dose (120 ml of 50 mM of GdDTPA per 30 g). The parameters of the sequences were as follows: T2w-3DRARE: TR = 1 s, TE = 75.8 ms, FA = 180°, BW = 100 Khz, Matrix size = 128³, FOV = 19.2 mm, Nav = 3. T1w-3D sPGRME: TR = 50 ms, TE = 4 ms, 4-echoes, with Echo spacing 4 ms, FA = 20°, BW = 50 Khz, Matrix size = 128³, FOV = 19.2 mm, Nav = 1. T2*w-3DGE: TR = 50 ms, TE = 4 ms, Echo number 5, Echo spacing 4 ms, FA = 20°, BW = 50 Khz, Matrix size = 128³, FOV = 19.2 mm, Nav = 1.

Results: Although the injected B16F10 melanoma cells successfully metastasized to the brain following intracarotid injection, their distribution was unexpected. Unlike what was reported by Perides et al., 100% of the induced tumors grew within the ventricles or meningeal space and not in the brain parenchyma (N = 8/8, Figure 1), thus confirming the findings by Fiddler et al. (4). Despite this non-clinical distribution, this model did induce multifocal tumors (Figure 2), reminiscent of aggressive late stage metastases. Such tumors are difficult to treat when observed clinically. The variability of the MRI contrast in these various foci was

similar to what is seen clinically showing edema (Figure 1), T1 brightening without contrast agent due to the presence of melanin (Figure 2), increased T1 brightening following contrast agent injection denoting excessive leakage within the metastatic lesion (Figure 4), as well as the associated susceptibility effect seen in T2* sequences (Figure 3), which is a unique feature used to diagnose metastatic brain melanoma (5).

Our MRI technique accurately revealed the extent of tumor growth and enabled the monitoring of changes in growth rates in vivo. Indeed, these tumors were first detected on post-operative week 3. These late starts to tumorigenesis, as well as the rapid growth of these tumors were both features that could only have been determined using MRI analysis. By comparing MRI scans obtained on the last stage of tumor growth with histopathology sections, we found that



meningial tumors were typically lost during sectioning and processing (Figures 5 and 6).

Conclusion: Due to the fact that our mMRI analyses are reminiscent of clinical radiological findings examining melanoma brain metastasis, our findings show that mMRI is a valuable tool to monitor metastatic brain tumorigenesis. Moreover, the dynamic information of tumor morphometry obtained using our longitudinal studies provided an accurate assessment of tumor size during tumorigenesis - an improvement over conventional single end point analysis representative of end stage histopathology studies.

Acknowledgments.

The authors Drs Elizabeth W. Newcomb, and David Zagzag for their help and advice at the initial stage of surgery. This work was supported in part by The Alice M. and Thomas J. Tisch Brain Tumor Research Fund and the Gruson Fund for Brain Tumor Research and Care to EBV and JGG, and by the Tilker Medical Research Foundation and the NYU Medical Center Applied Research Fund to YZW

References: 1)Jain R. et al. : Angiogenesis in brain tumours. Nature 8: 610-622(2007)

- 2) Perides G.et al.: The fibrinolytic system facilitates tumor cell migration across the blood-brain barrier in experimental melanoma brain metastasis. BMC Cancer 6:56 (2006)
- 3) Nieman B. et al.: Three-Dimensional, In Vivo MRI With Self-Gating and Image Coregistration in the Mouse. Magnetic Resonance in Medicine 61(5): 1148-1157
- 4) Fidler IJ. et al.: The biology of melanoma brain metastasis. Cancer and Metastasis Reviews 18:387-400(1999)
- 5) Gaviani P. et al.: Improved Detection of Metastatic Melanoma by T2*-Weighted Imaging. American Journal of Neuroradiology 27:605–08(2006)